Journal of Applied Polymer Science

Fabrication and characterization of novel zirconia filled glass fiber reinforced polyester hybrid composites

Muhammad Azeem Munawar,[1] Shahzad Maqsood Khan,[1] Nafisa Gull,[1] Muhammad Shafiq,[1] Atif Islam,[1] Saba Zia,[1] Aneela Sabir,[1] Awais Sattar Ghouri,[2] Muhammad Taqi Zahid Butt,[3] Tahir Jamil[1]

[1]Department of Polymer Engineering and Technology, University of the Punjab, Lahore 54590, Pakistan
[2]Department of Chemical Engineering, Engineering and Management Sciences, Takatu Campus, Balochistan University of Information Technology, Baleli, Quetta 87300, Pakistan
[3]Department of Metallurgy and Materials Engineering, College of Engineering and Emerging Technologies, University of the Punjab, Lahore 54590, Pakistan
Correspondence to: M. A. Munawar (E-mail: azeemicet119@gmail.com)

ABSTRACT: Novel hybrid glass fiber reinforced polyester composites (GFRPCs) filled with 1-5 wt % microsized zirconia (ZrO_2) particles, were fabricated by hand lay-up process followed by compression molding and evaluated their physical, mechanical and thermal behaviors. The consumption of styrene in cured GFRPCs was confirmed by Fourier transform infrared spectroscopy. The potential implementation of ZrO_2 particles lessened the void contents marginally and substantially enhanced the mechanical and thermal properties in the resultant hybrid composites. The GFRPCs filled with 4 wt % ZrO_2 illustrated noteworthy improvement in tensile strength (66.672 MPa) and flexural strength (67.890 MPa) while with 5 wt % ZrO_2 showed 63.93% rise in hardness, respectively, as compared to unfilled GFRPCs. Physical nature of polyester matrix for composites and an improved glass transition temperature (T_g) from 103 to 112 °C was perceived by differential scanning calorimetry thermograms. Thermogravimetric analysis revealed that the thermal stability of GFRPCs was remarkably augmented with the addition of ZrO_2. © 2016 Wiley Periodicals, Inc. J. Appl. Polym. Sci. **2016**, *133*, 43615.

KEYWORDS: composites; differential scanning calorimetry; mechanical properties; polyesters; properties and characterization

Received 23 December 2015; accepted 6 March 2016
DOI: 10.1002/app.43615

INTRODUCTION

Fiber reinforced polymer composites (FRPCs) are extensively employed in the construction, automobile, railway, military, power generation, marine, and aeronautic industries, mostly due to their high specific strength, ease of installation, electromagnetic transparency, noncorrodibility, and excellent mechanical properties.[1–3] FRPCs are multifunctional because they have always the opportunity of being tailored according to specific end-use applications.[4,5] FRPC comprises of a polymer which acts as a matrix and a reinforcing material which is selected as per desired applications and characteristics.[6] In conventional FRPCs, fiber acts as standard load carrying agent while the matrix is used to transfer the load to fiber and to shield it from any defect.[7] The special characteristics of E-glass fiber such as excellent dimensional stability, good resistance to corrosion and marvelous electrical insulation properties contribute significantly for reinforcement in FRPCs.[8] Thermoset resins such as epoxy, polyester, vinyl ester, polyurethane, phenolic resins, etc. have low viscosity, which can easily impregnate fiber as compared to the thermoplastic resins.[9] Unsaturated polyester resin (UPR) is frequently used with other constituents like fillers, reinforcements, initiators, accelerators, hardeners, etc. for the fabrication of composites due to its moderately low price and tremendous versatile properties of thermoset performance.[10]

The inclusion of inorganic fillers, such as ZnO, TiO_2, SiO_2, Al_2O_3, $Mg(OH)_2$, and $CaCO_3$ as third constituent in FRPCs, improve the fiber-matrix interface circumstances and also reduce porosity, brittle failure and misalignment of fibers.[11] The appropriate size, shape, specific surface area, concentration, and distribution of fillers contribute to significant improvement in physical, mechanical, and thermal properties of hybrid particulate filled FRPCs.[12] The interaction between composite matrix and filler is generally substantial when energy dissipation activities are energetic during plastic deformation and fracture behavior.[13,14]

$CaCO_3$ filler is inexpensive, nontoxic, and biocompatible which enhances mechanical as well as thermal characteristics in GFRPCs but decreases hardness.[15] ZrO_2 is a metallic oxide and

© 2016 Wiley Periodicals, Inc.

polymorphic in nature; it reveals a different equilibrium (stable) crystal structure at varying temperatures having no alteration in chemistry.[16] It has exceptional physical, optical, dielectric, chemical, mechanical, and thermal properties such as; excellent transparency in visible and adjacent infrared region, good refractive index, large optical band gap, low optical loss, high dielectric constant, good chemical stability, excellent wear resistance, elevated melting point, and high resistance to thermal shock. ZrO_2 addition in polymeric materials enhances mechanical and thermal stability especially hardness of GFRPCs.[17,18]

FRPCs are anisotropic and have structural heterogeneity with unavoidable internal manufacturing defects, such as porosity, brittle failure and high deformability, misalignment of fibers or bad stack of the prepreg layers of laminated composites.[19] These defects lead to mechanical and thermal instability of resultant composites and do not permit complete exploitation of the material's strength. In order to lessen these delinquents of FRPCs, several authors have proposed particulate filled FRPCs.[20,21] Satheesh et al. have investigated the tribological properties of FRPCs filled with fly ash filler. They found improved tensile, flexural, compression and hardness properties with increasing fly ash concentration.[22] Madugu et al. concluded that by increasing the amount of iron filler in the glass/polyester resulted in an improvement of 77.8, 30, and 37.55% in the hardness, density and shrinkage values, respectively.[23] M.K Hossain investigated that incorporation of CNFs into the glass/polyester composites resulted in better thermal stability.[24] Hybrid FRPCs are renowned for their synergic effects on cost reduction and development in stiffness even up to three times of their magnitude.[25]

The objective of the current research work was to fabricate a novel class of hybrid GFRPCs filled with 1–5 wt % microsized ZrO_2 filler particles by hand lay-up technique followed by compression molding. The influence of ZrO_2 particles on physical, mechanical, and thermal behaviors of synthesized GFRPCs was explored and it is recommended to be used in construction, automobile, and aeronautic industries.[12,26–28]

EXPERIMENTAL

Materials

Micro-ZrO_2 particles (melting point ~2715 °C and 5.68 g/cm^3 density) were purchased from BDH Chemicals Ltd Poole England. E-glass fiber roving strand mat was obtained from Taishan Fiberglass Inc., China. Unsaturated polyester resin (with 42% styrene contents and 3% fumed silica flash point 35 °C, density: 1.11–1.23 g/cm^3), cobalt naphthanate and methyl ethyl ketone peroxide (MEKP) were acquired from local commercial market and were used in this study without any pretreatment.

Method

The dispersion of ZrO_2 filler with distinct weight compositions (1–5 wt %) in UPR were obtained at 1500 rpm for 30 min through high Dispersing Machine (IKA Ultra-Turrax TV45H, Nr. 4247, Disperser Homogenizer). After cooling of dispersion at 30 °C, 1 wt % MEKP catalyst was added, followed by the addition of 0.5 wt % cobalt naphthenate accelerator to initiate and promote the curing of UPR prior to adhere with reinforcement phase. The mixture was stirred to mix the catalyst and accelerator in ZrO_2-UPR dispersion. To make composite laminates, four layers of cross-plied woven roving E-glass fiber mat with dimensions of 175 × 175 mm were placed separately on aluminum foil at work table. ZrO_2-UPR dispersion containing catalyst and accelerator was poured on these layers uniformly using hand-lay-up technique. Finally, the completely impregnated layers were stacked on one another and wrapped in aluminum foil and placed between two stainless steel (SS) sheets. The whole assembly of composite laminates (along with SS sheets) was cured and molded by High Temperature Melt Press (HTMP) machine under pressure of 4 Metric Ton (M.Ton) at 60 °C for 60 min to obtain complete curing reaction and uniform thickness of ZrO_2 filled composite laminates. At the end of each process, before removing the composite laminates out of the HTMP platens as final product, the entire assembly was cooled gradually to room temperature and the pressure was kept constant in order to diminish the thermal residual stresses. All composites laminates of ZrO_2 filled and unfilled were manufactured with the same approach. The formulations of composite specimens with different wt % ZrO_2 is shown in Table I and the pictorial view of fabrication of GFRPCs is illustrated in Figure 1.

Table I. Codes for Composite Specimens with Detailed Composition

Code names for composites	Matrix content dispersed with ZrO_2 (wt %)	Fiber content (wt %)	Dispersed ZrO_2 content in matrix (wt %)
GFRPC-0	50	50	0
GFRPC-1	50	50	1
GFRPC-2	50	50	2
GFRPC-3	50	50	3
GFRPC-4	50	50	4
GFRPC-5	50	50	5

CHARACTERIZATION

Fourier Transform Infrared Spectroscopy

Spectra of GFRPCs were recorded by IR Prestige-21 (Shimadzu) employing the attenuated total reflectance (ATR) accessary

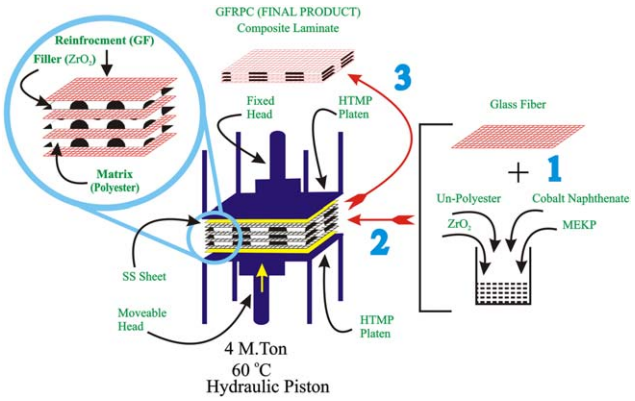

Figure 1. Pictorial view of fabrication of GFRPCs. [Color figure can be viewed in the online issue, which is available at wileyonlinelibrary.com.]

having zinc selenide (ZnSe) crystal. The air background of the instrument was run before each test of composite. The wavenumber range was from 4000 to 600 cm^{-1} at 100 scans per spectrum and resolution of 4 cm^{-1}.

Density and Void Fraction

The theoretical density of composites was determined by using the rule of mixture as proposed by Broutman and Agarwal[29] in eq. (1).

$$\rho_{ct} = \frac{1}{\left(\frac{W_f}{\rho_f}\right) + \left(\frac{W_m}{\rho_m}\right)} \quad (1)$$

Where as W and ρ demonstrate weight fraction and density of constituents, respectively. The suffix f, m, and ct represent the fiber, matrix, and the composite material, respectively. Since ZrO_2 filled GFRPCs comprised matrix, fiber and particulate filler, hence the eq. (1) can be tailored as eq. (2).

$$\rho_{ct} = \frac{1}{\left(\frac{W_f}{\rho_f}\right) + \left(\frac{W_m}{\rho_m}\right) + \left(\frac{W_p}{\rho_p}\right)} \quad (2)$$

Where, the suffix p reveals the specific filler constituents. The actual density of the composite was determined by using Archimedes′ principle.[20] The void volume fraction (V_v) in composite was computed with eq. (3).

$$V_v = \rho_{ct} - \rho_{ce} / \rho_{ct} \times 100 \quad (3)$$

Linear Shrinkage

The dimensions of GFRPCs (i.e., length, width, and thickness) were calculated immediately before the curing. After curing, the dimensions were also noted. The difference in thickness in percentage gave the linear shrinkage of the specimens.[23]

$$\text{Linear Shrinkage} = \frac{t_1 - t_2}{t_1} \times 100 \quad (4)$$

Where t_1 is initial thickness (mm) after prepartion of laminated sample and t_2 is final thickness (mm) after curing.

Tensile Strength

Universal Testing Machine (UTM), Testometric Model FS100 CT UK with 100 KN load cell was used to determine the tensile behavior under a static load. Test samples for tensile properties with end tabs were fabricated according to ASTM: D 3518-0 having dimensions (200 × 25 × 2.5 mm). The UTM was operated at a speed of 2.0 mm/min at ambient temperature conditions during tensile testing. Five individual samples for all composites were manufactured for both tensile testings.

Hardness

Hardness of test samples with dimensions (25.4 × 25.4 × 2.5 mm) was determined using a Bench Rockwell Hardness Tester Model NR3-DR Ernst Switzerland following ASTM: D785-08. The Brinell hardness number (HB) is determined by the formula:

$$HB = 2F/\{3.14D \times [D - (D2 - Di2)1S/2]\}$$

Where, F is applied load in kp (kilo pound), D is indenter diameter (mm), and Di is indentation diameter (mm). A carbide ball indenter with spherical base of 2.5 mm diameter D was penetrated into the material under applied load F. Preload was 1000 kp while applied load was 62.5 kp with ratio HB10. In Brinell principle, F/D2 is a fundamental ratio between applied load and indenter diameter for determining hardness and HB10 is ratio of 2.5 mm ball and 62.5 kp load. Brinell hardness was noted at ten different places on the specimen.[30]

Thermogravimetric Analysis/Differential Scanning Calorimetry

Simultaneous differential scanning calorimetry/thermogravimetric analyzer (SDT) Model Q600 of TA Instrument USA was used to perform differential scanning calorimetry (DSC) and thermogravimetric analysis (TGA) of fabricated composites. Thermal behavior of each sample (~10 mg) was observed at a constant heating rate of 10 °C/min from 35 to 800 °C in nitrogen atmosphere with purging rate of 20 mL/min.

Scanning Electron Microscopy

Scanning electron micrographs of ZrO_2 filled and unfilled GFRPCs were obtained using a JEOL (JSM-6480LV) microscope to analyze the morphology, filler distribution, and surface properties of the composites. The low vacuum mode was used to operate GFRPC at 20 kV while the morphology was observed at magnification of ×500.

RESULTS AND DISCUSSION

The crosslinking of UPR and the hydrogen bonding of zirconia and silica content of glass fiber during the synthesis of micro-sized ZrO_2 filled GFRPCs is shown in the following proposed Scheme 1. UPR chains were crosslinked due to reactive —C=C— bonds via vinyl group of styrene in the presence of MEKP catalyst and cobalt naphthenate accelerator. The three dimensional rigid network of cured unfilled and ZrO_2 filled GFRPCs were the outcome of crosslinking (physical and chemical) between polyester chains, ZrO_2 and SiO_2 constituents of glass fiber.

Fourier Transform Infrared Spectroscopy

The infrared analysis of UPR, GFRPC-0 to GFRPC-5 is shown in Figure 2. The IR spectrum of UPR before curing reaction exhibited a strong asymmetric stretching band at 1258.08 cm^{-1} which confirmed the existence of —C—O—C— ester linkage. The bands at 701.42 cm^{-1} (—CH— out of plane bending in benzene ring) and 907.88 cm^{-1} (—C=C— group) were typical of styrene however band at 1723.70 cm^{-1} [carbonyl stretching in ester linkage (—C—O—CO—)] was characteristics of polyester. A weak stretching band at 1642.30 cm^{-1} and out of plane bending at 982.45 cm^{-1} were ascribed to —C=C— group of polyester. The —CH stretching was confirmed by the existence of band at 2958.27 cm^{-1}. –Si-O band in UPR was observed at 1071.11 cm^{-1} which was shifted to 1068.65 cm^{-1} (GFRPC-0 to GFRPC-5) due to hydrogen bonding with —CH group of polyester chain (Scheme 1).

The disappearance of —C=C— band at 907.88 cm^{-1} endorsed the curing process in terms of consumption of styrene in cured GFRPCs. The out of plane band at 982.45 cm^{-1} was vanished in GFRPC-0 having no filler (ZrO_2) content and also in GFRPC-1 to GFRPC-5. The —CH stretching band at 2958.27 cm^{-1} became sharper as noticed in cured GFRPC-0

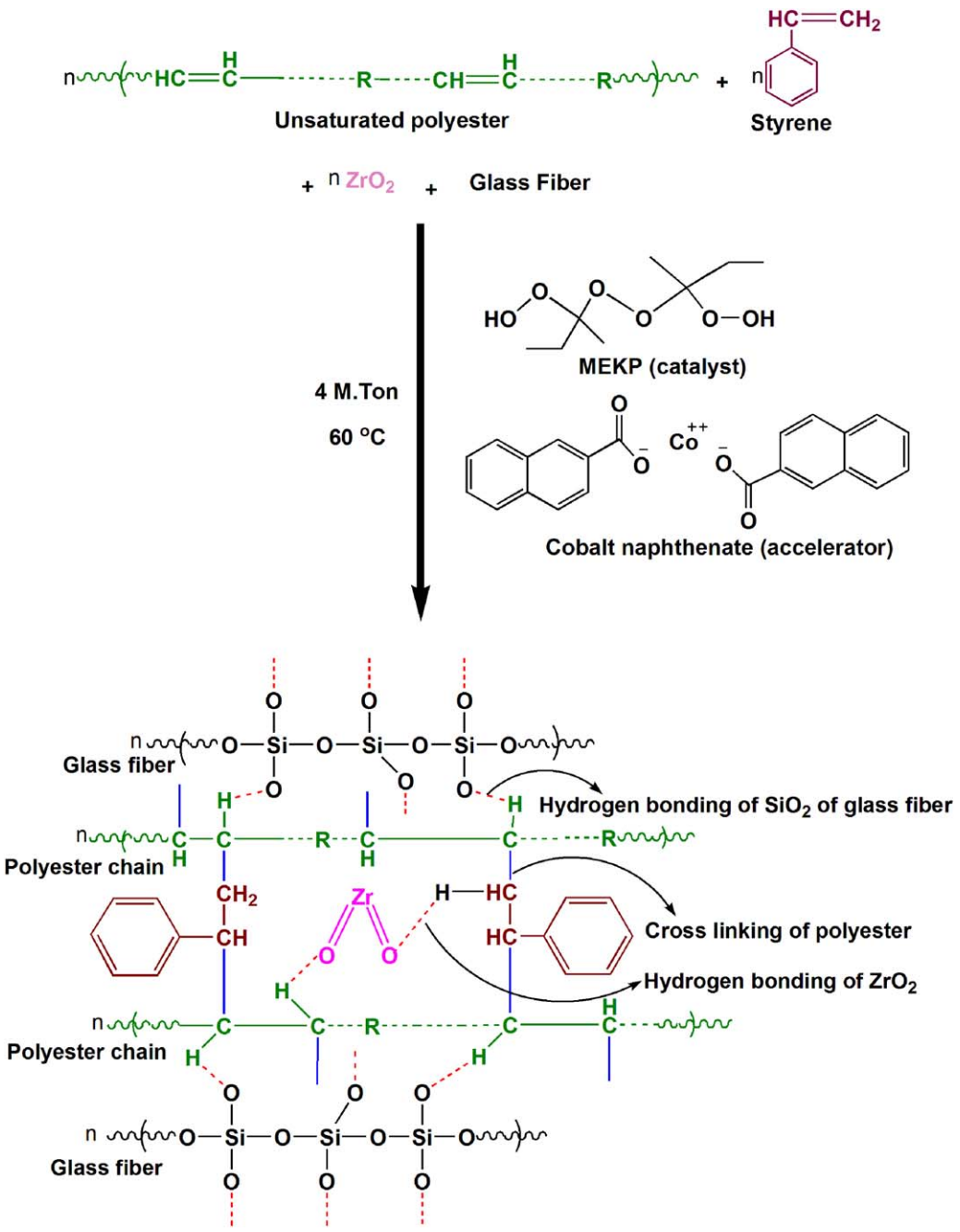

Scheme 1. Proposed scheme for the fabrication of GFRPCs. [Color figure can be viewed in the online issue, which is available at wileyonlinelibrary.com.]

which was shifted to 2947.88 cm^{-1} in ZrO_2 filled composites i.e. GFRPC-1 to GFRPC-5. The —CH stretching band was moved toward lower wavenumber (2958.27 to 2947.88 cm^{-1}) due to the hydrogen bonding with the addition of zirconia filler and silica content (Scheme 1). The stretching band at 1642.30 cm^{-1} (UPR) was observed at 1647.66 cm^{-1} in cured GFRPC-0 and almost disappeared in composite having ZrO_2 content from 1 to 5 wt % (GFRPC-1 to GFRPC-5) as shown in Scheme 1. This ratified the conversion of this group to alkane through crosslinking process which was accredited to the contribution of —HC═CH— functional group during the curing process.[31–33]

Density and Void Contents

Theoretical and actual densities of composite specimens accompanied by their equivalent void volume fractions are illustrated in Table II. It was observed that void volume fraction in GFRPC-0 was 3.67% whereas it declined from 3.48 to 2.39% in $GFRPC_s$ with ZrO_2 (1–4 wt %) addition. The reduction of void volume fractions was the consequence of suitable interfacial bonding between filler and matrix and homogeneity in the composite. The applied pressure on the laminates with HTMP of 4 M.Ton also led to suppressing the formation of voids in the resultant hybrid composites.[34] The increasing trend in voids formation beyond 4 wt % ZrO_2 loading was due to high

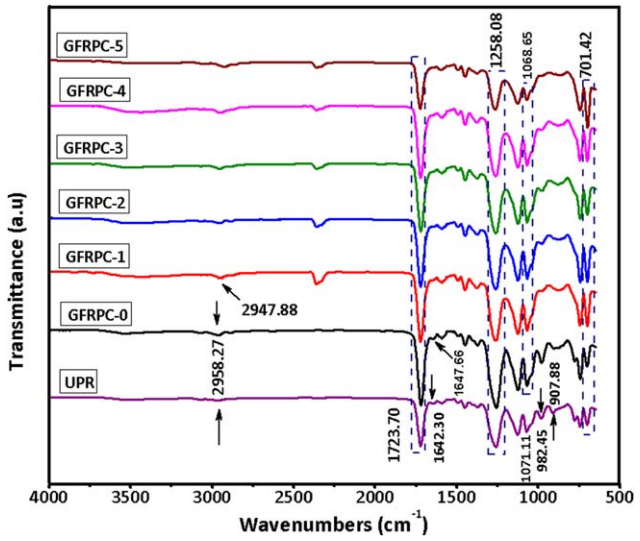

Figure 2. FTIR spectra of UPR and GFRPC-0 to GFRPC-5. [Color figure can be viewed in the online issue, which is available at wileyonlinelibrary.com.]

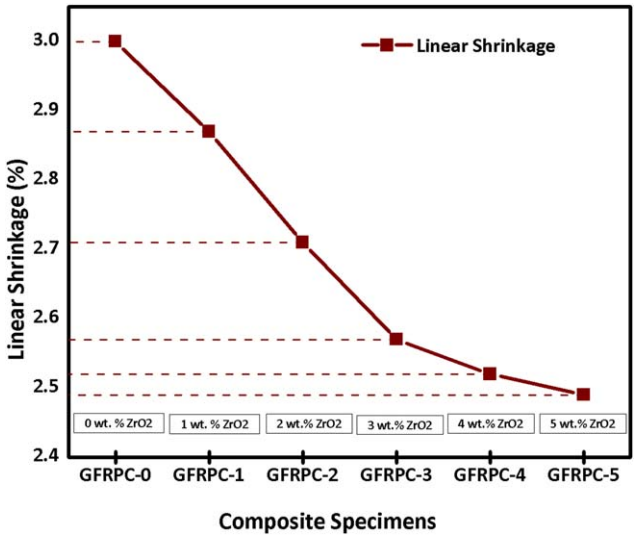

Figure 3. Variation of linear shrinkage of GFRPCs with increasing wt % of ZrO_2. [Color figure can be viewed in the online issue, which is available at wileyonlinelibrary.com.]

intensification of viscosity in resin system at high concentration of filler which caused heterogeneity and agglomeration of ZrO_2 particles in GFRPC-5 composites.[35–37]

Linear Shrinkage

A monotonous reduction in volume shrinkage was observed for GFRPCs with increasing ZrO_2 filler in Figure 3. This may be accredited to the fact that shrinkage during curing process was decreased as the weight concentration of ZrO_2 filler in resin matrix increased.[23] The addition of ZrO_2 filler increased the viscosity of UPR and formed interface between filler and polyester. The phase separation between filler and matrix is related not only to the chemical structure, molecular weight and dipole moment of filler but also to the structure and composition of UPR and styrene.[38] The interface between filler and polyester delayed the cure rate mechanism. The delayed process was the consequence of better hydrogen bonding and cross linking network between filler and UPR and decreased the entrapment of air bubbles thus decreased the shrinkage volume of ZrO_2 filled GFRPCs.[39]

Tensile Test

It was observed from Figure 4 that both the tensile strength and modulus of GFRPCs were improved with an increase in ZrO_2 loading up to maximum of 4 wt %. The specimens having 4 wt % ZrO_2 content exhibited maximum value of 66.672 MPa and 6.901 GPa for tensile strength and modulus, respectively, and then decreased beyond 4 wt % ZrO_2 filler. It was noted that 4 wt % ZrO_2 was the key concentration for good tensile properties of hybrid ZrO_2 filled GFRPCs. The enhancement in the tensile properties was the consequence of formation of bonds (physical and chemical) in the interfacial region between GFRPCs and ZrO_2 particles.[40] The value of interfacial bonding in the particulate filled GFRPCs mainly depend upon the optimized composition of matrix, fiber and filler particles. When matrix and particles were well connected, the applied stress was efficiently transferred from matrix to the particles resulting in high strength[22,41] having conformity with the recent research.[23] The reduction in tensile properties of GFRPCs above 4 wt % ZrO_2 was owing to uneven dispersion of the ZrO_2 particles that has increased the number of voids, or voids of larger diameter. Voids were responsible of stress concentration, which initiated crack growth and resulting in reduced tensile-mechanical properties.[42,43] GFRPC-5 showed 78.05% and 19.911% decrease in tensile strength and tensile modulus with an increase of 0.43% void contents in GFRPC-5 relative to GFRPC-4[44] as shown in Figure 4 and Table II.

Table II. Theoretical Density, Actual Density and Void Volume Fraction of GFRPC-0 to GFRPC-5 Composites

Composite specimens	Theoretical density (gm/cc) mean (std. deviation)	Actual density (gm/cc) mean (std. deviation)	Void volume fraction (%)
GFRPC-0	2.042 (0.03)	1.967 (0.05)	3.67
GFRPC-1	2.043 (0.05)	1.972 (0.06)	3.48
GFRPC-2	2.043 (0.01)	1.980 (0.04)	3.08
GFRPC-3	2.045 (0.05)	1.986 (0.06)	2.89
GFRPC-4	2.047 (0.04)	1.998 (0.03)	2.39
GFRPC-5	2.051 (0.05)	1.993 (0.04)	2.82

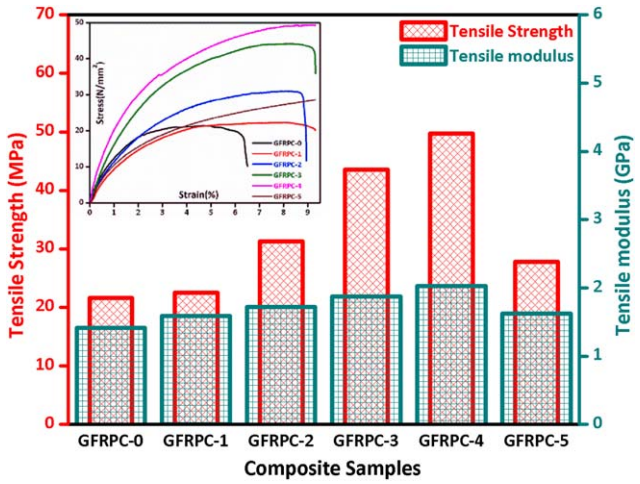

Figure 4. Tensile strength and tensile modulus results of GFRPC-0 to GFRPC-5. [Color figure can be viewed in the online issue, which is available at wileyonlinelibrary.com.]

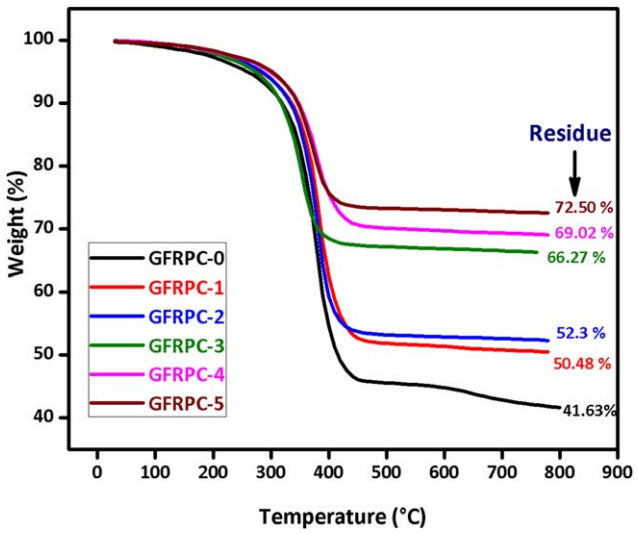

Figure 6. TGA Thermograms of GFRPC-0 to GFRPC-5. [Color figure can be viewed in the online issue, which is available at wileyonlinelibrary.com.]

Hardness

The weakness of thermosetting resins is their poor resistance to penetration, but inorganic particles are effective toughenners for thermosetting resins.[45] The variations in the Brinell Hardness Values (BHV) of filled and unfilled GFRPCs are illustrated in Figure 5. This figure showed that the hardness of GFRPCs increased linearly with the increase in ZrO_2 concentration. GFRPC-5 exhibited 63.93% increase in hardness as compared to unfilled one (GFRPC-0). Hemalata Jena and coworkers have reported the same research work.[46] The reason behind high resistance in penetration or increased hardness was accredited to the fact that when compressive stress was applied by HTMP on the prepreg sample and all phases of matrix, fiber, and filler were contacted with one another more effectively. Therefore, interface has transmitted pressure more superbly although the interfacial bond might be weak.[4,26,36] During the applied compression load, the inter particle distance is decreased which results in increased hardness.[47] It was also significant that the matrix content was decreased with increase in the concentration of ZrO_2 ceramic particles in the system which donated their inherent hardness to GFRPCs. The impact and hardness analysis in present study depicted that ZrO_2 will be a promising filler in future composites.

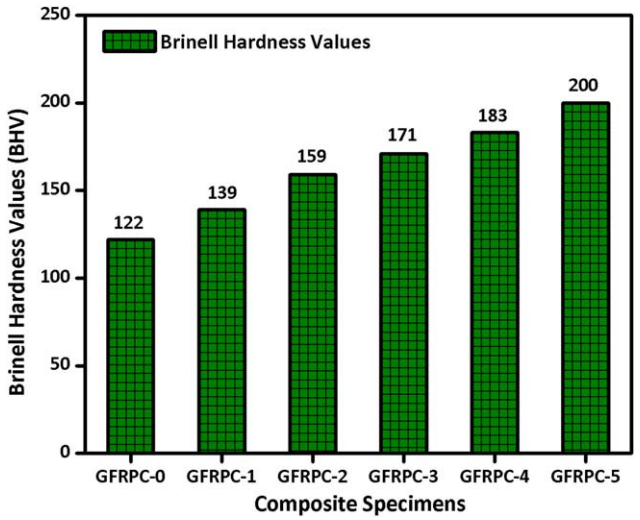

Figure 5. Hardness results of GFRPC-0 to GFRPC-5. [Color figure can be viewed in the online issue, which is available at wileyonlinelibrary.com.]

Thermogravimetric Analysis

TGA of unfilled and ZrO_2 filled GFRPCs was recorded to estimate the thermal stability of specimens (Figure 6). During TGA, weight of the analyzed material decreases due to the decomposition or volatilization while increases in weight occur due to the gas absorption or some chemical reaction.[48] Thermal decomposition profiles of unfilled and ZrO_2 filled GFRPCs showed weight losses in different steps. The weight loss started from room temperature to 100 °C in composite specimens was attributed to the elimination of moisture,[49] whereas dehydration occurred in temperature range of 100–285 °C.[50] The onset of degradation of unfilled and ZrO_2 filled GFRPCs was started at 285 °C while higher decomposition rate was associated with scission of weak bonds. The unzipping of highly strained cross-linked chains was occurred above 300 °C and converted in to straight chains. All linear polymer backbone chains decomposed

Table III. Thermal Decomposition Data of Unfilled and ZrO_2 Filled GFRPCs at Various Percentages Weight Loss

Composite specimens	$T_{10\%}$[a] °C	$T_{30\%}$ °C	Residue[b] %
GFRPC-0	315	375	41.63
GFRPC-1	332	386	50.48
GFRPC-2	335	393	52.3
GFRPC-3	337	407	66.27
GFRPC-4	348	523	69.02
GFRPC-5	343	750	72.5

[a] $T_{10\%}$ and $T_{30\%}$ are the temperatures at 10% and 30% weight losses.
[b] Residue at 800 °C.

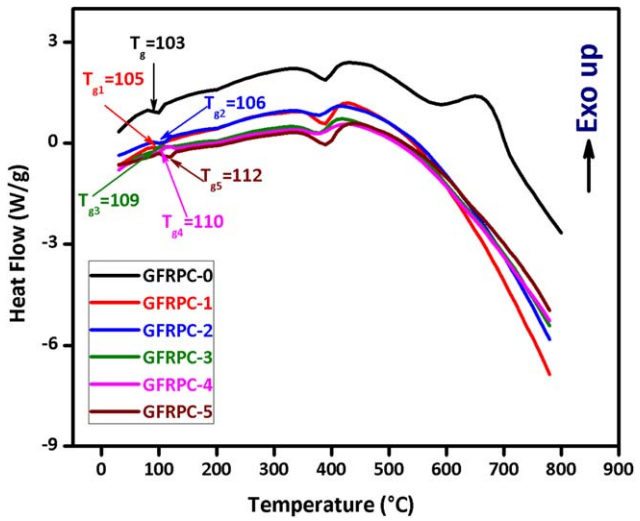

Figure 7. DSC curves of GFRPC-0 to GFRPC-5. [Color figure can be viewed in the online issue, which is available at wileyonlinelibrary.com.]

into small fragments at 410 °C near offset temperature.[51,52] The residue left behind at 800 °C was attributed to the amount of glass fiber and ZrO_2 after the entire burning of polyester matrix. It was determined from this analysis that the unfilled GFRPC-0 exhibited the weight loss up to 58.37%, which was limited to 27.5% for GFRPC-5. The thermal decomposition data of composites at various percentages of weight losses is represented in Table III. This confirmed that 10 and 30 wt % losses of GFRPC-0 was at 315 and 375 °C which was increased up to 343 and 750 °C in GFRPC-5, respectively. This data also elucidated that as the decomposition temperature was marginally enhanced, the overall weight loss of composite materials decreased and residue contents increased with the increase in wt % of ZrO_2. The higher thermal stability of GFRPC-5 as compared to GFRPC-0 was due to improved interlocking of polyester chains with ZrO_2 in the presence of MEKP hardener. Thus, interlocking reduced the segmental motion of polyester chains on heating. When heating temperature gradually increased, the interface between matrix and filler prompted to weaken which

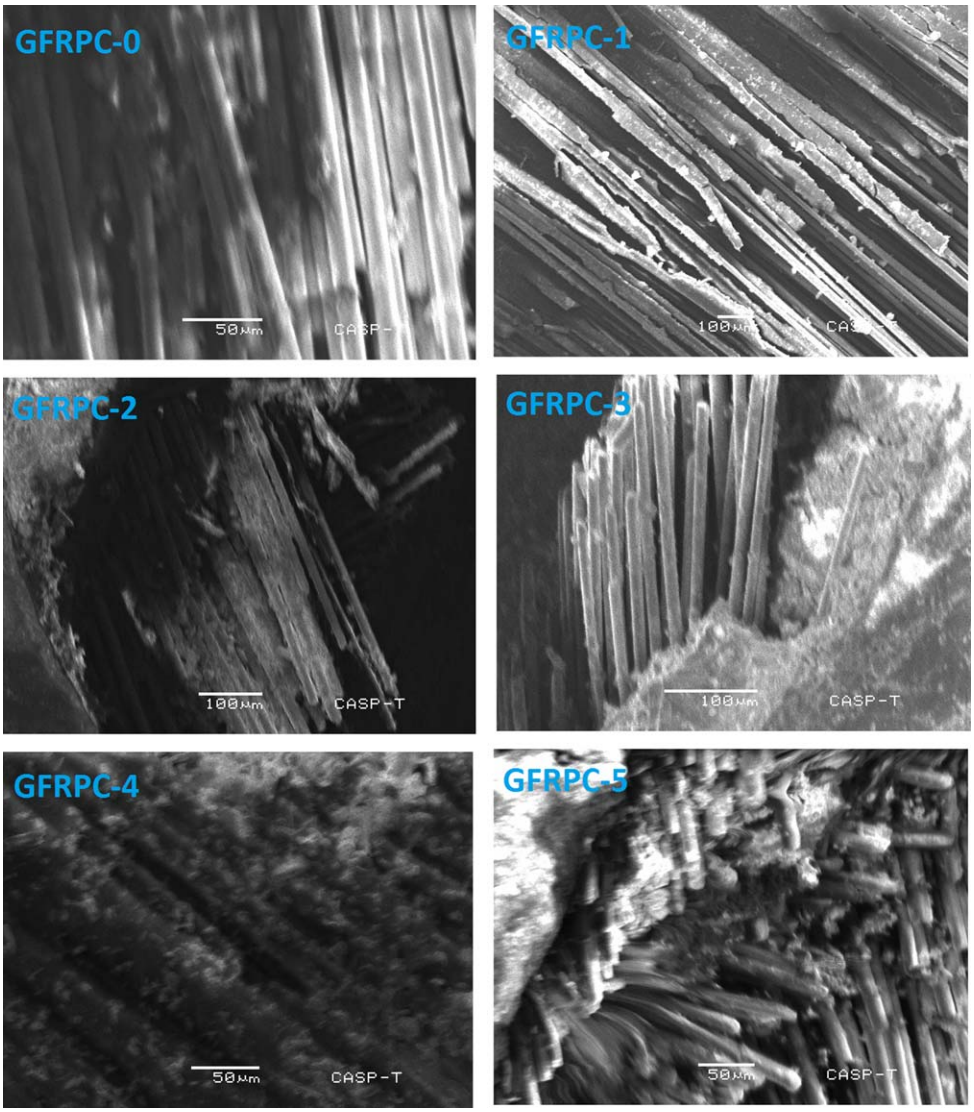

Figure 8. SEM images of fractured surfaces views of GFRPCs with 0, 1, 2, 3, 4, and 5 wt % ZrO_2 filler dispersion in matrix. [Color figure can be viewed in the online issue, which is available at wileyonlinelibrary.com.]

triggered the mobility of molecular chains drastically, ultimately composites decomposed at higher temperatures. This finding is in accordance with the study by Hossain and coworkers.[24]

Differential Scanning Calorimetry

DSC interpretation (Figure 7) showed that the glass transition temperature (T_g) of cured unfilled GFRPC-0 composite shifted to higher temperature with an increase in ZrO_2 content. The T_g of GFRPC-0 and GFRPC-5 were 103 and 112 °C, respectively, showing an increase in the T_g of composites. Increment in T_g (9 °C) for GFRPCs was the consequence of an enhanced crosslinking density,[24,53] which developed high mechanical reinforcement from ZrO_2 crystalline morphology and restricted segmental motion of chain segments near the filler particles.[20,54] Thus, ZrO_2 filled GFRPCs can be exercised at higher temperatures than unfilled GFRPC-0. The large endothermic peaks around 400 °C were the decomposition temperatures of unfilled and ZrO_2 filled GFRPCs which were also justified in TGA analysis.

Scanning Electron Microscopy

SEM images depict the filler dispersion in polymer matrix more visually. The Figure 8 shows that, when the contents of ZrO_2 are 1 and 2 wt %, they have little difference in their dispersions state, and a filler network is poor in both GFRPC-1 and GFRPC-2 composites. But in GFRPC-3 and GFRPC-4, ZrO_2 filler are more uniformly dispersed with little aggregation and filler network is also stronger than that in GFRPC-1 and GFRPC-2. The ZrO_2 filled GFRPCs led to the formation of packed chain structure by the formation of filler network with unsaturated polyester resin as observed in the GFRPC-3 and GFRPC-4. The GFRPC-5 with high ZrO_2 content (5 wt %) showed an entanglement behavior. Moreover, glass fibers which are used as a reinforcement of GFRPCs can be also observed. These SEM images proved that appropriate filler concentration can significantly suppress the entanglement and aggregation of GFRPCs, consequently leading to excellent mechanical and thermal properties.[55,56]

CONCLUSIONS

It was concluded from this research that physical, mechanical, and thermal properties of GFRPCs were improved with the incorporation of microsized ZrO_2 filler. FTIR analysis confirmed the utilization of styrene and the participation of —HC═CH— functional group during crosslinking process. The higher concentration of ZrO_2 (4 wt %) led to the significant decrease in void volume fraction compared to unfilled one (GFRPC-0). A monotonous reduction in volume shrinkage of GFRPCs was observed by increasing filler concentration. Tensile strength and modulus were enhanced by filler loading up to 4 wt % with subsequent reduction above this concentration while hardness was improved gradually by increase in ZrO_2 content in GFRPCs. The residue content in TGA analysis showed that GFRPC-5 has the highest residue amount as compared to other GFRPCs. T_g was improved from 103 to 112 °C with increase in the filler concentration. Hence, it was inferred that microsized ZrO_2 was a promising filler for incremental assessment in physical, mechanical and thermal properties of GFRPCs. From above discussed results of physical, thermal, and mechanical properties, it is recommended that these composites can be used for high strength and high temperature applications.

ACKNOWLEDGMENTS

We are highly obliged to Department of Polymer Engineering and Technology, University of the Punjab, Lahore, Pakistan for help in execution of this research project regarding all phases of synthesis and characterization. Authors Contribution: Engr. Muhammad Azeem Munawar has fabricated the composites, contributed in analysis of all physical, thermal and mechanical characterizations and written the manuscript. Engr. Shahzad Maqsood Khan guided in the performance of thermal and mechanical experiments, sketched the graphical abstract of the manuscript and helped in proof reading of final manuscript and response to the referees comments. Miss Nafisa Gull helped in fabrication of samples, sketched the SEM image and helped in proof reading of final manuscript and response to the referees comments. Engr. Muhammad Shafiq contributed in testing of the samples regarding Mechanical properties of the prepared composites. Dr. Atif Islam guided in the interpretation of all thermal, mechanical and FTIR analysis of composites, helped in proof reading of final manuscript and response to the referees comments. Miss Saba Zia assisted in testing of the thermal analysis of prepared composites. Engr. Aneela Sabir served in interpretation of SEM analysis of samples and in proof reading of the manuscript. Engr. Awais Sattar Ghouri helped us in physical characterization of the prepared samples and in the correction of grammatical mistakes in the manuscript. Prof. Dr. Muhammad Taqi Zahid Butt supervised the research work and provided all the required facilities for the execution of this project. Prof. Dr. Tahir Jamil is the most senior among all authors who supervised this research work in all aspects including synthesis, characterization and paper write-up process.

REFERENCES

1. Gonilha, J. A.; Barros, J.; Correia, J. R.; Sena-Cruz, J.; Branco, F. A.; Ramos, L. F.; Gonçalves, D.; Alvimc, M. R.; Santos, T. *Compos. Struct.* **2014**, *118*, 496.
2. Ramesh, M.; Palanikumar, K.; Reddy, K. H. *Compos. Part B* **2013**, *48*, 1.
3. Arun, K. R.; Alok, S. *Mater. Des.* **2012**, *41*, 131.
4. Chauhan, S. R.; Thakur, S. *Mater. Des.* **2013**, *51*, 398.
5. Meira, C. A.; Ribeiro, M. S.; Santos, J.; Meixedo, J. P.; Silva, F. J.; Fiuza, A.; Dinis, M. L.; Alvim, M. R. *Constr. Build. Mater.* **2013**, *45*, 87.
6. Liu, D.; Tang, Y.; Cong, W. L. *Compos. Struct.* **2012**, *94*, 1265.
7. Nirmal, U.; Hashim, J.; Ahmad, M. *Tribol. Int.* **2015**, *83*, 77.
8. Adam, K.; Senthil, K. *J. Manuf. Processes* **2011**, *13*, 67.
9. Mishra, S.; Mohanty, A. K.; Drzal, L. T.; Misra, M.; Parija, S.; Nayak, S. K.; Tripathy, S. S. *Compos. Sci. Technol.* **2003**, *63*, 1377.
10. Morote-Martínez, V.; Pascual-Sánchez, V.; Martín-Martínez, J. M. *Eur. Polym. J.* **2008**, *44*, 3146.

11. Karimi, M.; Habibi-Rezaei, M.; Safari, M.; Moosavi-Movahedi, A. A.; Sayyah, M.; Sadeghi, R.; Kokini *J. Food Res. Int.* **2014**, *66*, 485.
12. Gull, N.; Khan, S. M.; Munawar, M. A.; Shafiq, M.; Anjum, F.; Butt, M. T. Z.; Jamil, T. *Mater. Des.* **2015**, *67*, 313.
13. Detomi, A. C.; Santos, R. M.; Filho, S. L. M. R.; Martuscelli, C. C.; Panzera, T. H.; Scarpa, F. *Mater. Des.* **2014**, *55*, 463.
14. Uddin, M. F.; Sun, C. T. *Compos. Sci. Technol.* **2008**, *68*, 1637.
15. Patel, V. K.; Dhanola, A. *Int. J. Eng. Sci. Technol.* (in press) DOI: 10.1016/j.jestch.2015.10.005
16. Zhang, Y.; Zhang, J. *Mater. Today Proc.* **2014**, *1*, 44.
17. Srikanth, I.; Padmavathi, N.; Kumar, S.; Ghosal, P.; Kumar, A.; Subrahmanyam, C. *Compos. Sci. Technol.* **2013**, *80*, 1.
18. Stojadinović, S.; Vasilić, R.; Radić, N.; Grbić, B. *Opt. Mater.* **2015**, *40*, 20.
19. Chowdhury, N. T.; Wang, J.; Chiu, W. K.; Yan, W. *Compos. Struct.* **2016**, *135*, 61.
20. Firdosh, S.; Murthy, H. N.; Pal, R.; Aganadi, G.; Raghavendra, N.; Krishna, M. *Compos. Part B* **2015**, *69*, 443.
21. Harizi, W.; Chaki, S.; Bourse, G.; Ourak, M. *Compos. Part B* **2015**, *70*, 131.
22. Raja, S. R.; Manisekar, K.; Manikandan, V. *Mater. Des.* **2014**, *55*, 499.
23. Madugu, I. A.; Abdulwahab, M.; Aigbodion, V. S. *J. Alloy. Compd.* **2009**, *476*, 807.
24. Hossain, M. K.; Hossain, M. E.; Dewan, M. W.; Hosur, M.; Jeelani, S. *Compos. Part B* **2013**, *44*, 313.
25. Hartikainen, J.; Hine, P.; Szabo, J. S.; Lindner, M.; Harmia, T.; Duckett, R. A.; Friedrich, K. *Compos. Sci. Technol.* **2005**, *65*, 257.
26. Patnaik, A.; Satapathy, A.; Mahapatra, S. S.; Dash, R. *J. Reinf. Plast. Compos.* **2009**, *28*, 1305.
27. Sadeghian, R.; Gangireddy, S.; Minaie, B.; Hsiao, K.-T. *Compos. Part A* **2006**, *37*, 1787.
28. Bakis, C.; Bank, L.; Brown, V.; Cosenza, E.; Davalos, J.; Lesko, J.; Machida, A.; Rizkalla, S.; Triantafillou, T. *J. Compos. Constr.* **2002**, *6*, 73.
29. Agarwal, B. D.; Broutman, L. J.; Chandrashekhara, K. Analysis and Performance of Fiber Composites, 3rd ed.; Wiley: Hoboken, New Jersey, USA, **2006**; p 562.
30. Leyi, G.; Wei, Z.; Jing, Z.; Songling, H. *Measurement* **2011**, *44*, 2129.
31. Cao, X.; Lee, L. *J. Polym.* **2003**, *44*, 1893.
32. Huang, Y.-J.; Leu, J.-S. *Polymer* **1993**, *34*, 295.
33. Huang, Y.-J.; Wen, Y.-S. *Polymer* **1994**, *35*, 5259.
34. Eom, Y.; Boogh, L.; Michaud, V.; Sundarland, P.; Manson, J-AE. **1999**.
35. Aktas, L.; Dharmavaram, S.; Hamidi, Y. K.; Altan, M. C. *J. Compos. Mater.* **2008**, *42*, 2209.
36. Biswas, S.; Satapathy, A. *Tribol. Trans.* **2010**, *53*, 520.
37. Patnaik, A.; Satapathy, A.; Mahapatra, S. S.; Dash, R. *J. Reinf. Plast. Compos.* **2008**, *27*, 1093.
38. Li, W.; Lee, L. J.; Hsu, K. H. *Polymer* **2000**, *41*, 711.
39. Huang, Y. J.; Liang, C. M. *Polymer* **1996**, *37*, 401.
40. Pothan, L. A.; Oommen, Z.; Thomas, S. *Compos. Sci. Technol.* **2003**, *63*, 283.
41. Yunus, R. B.; Zahari, N. H.; Salleh, M. A.; Ibrahim, N. A. *Key Eng. Mater.* **2011**, *471*, 652.
42. Judd, N. C.; Wright, W. *Sampe. J.* **1978**, *14*, 10.
43. Won, J. P.; Yoon, Y. N.; Hong, B. T.; Choi, T. J.; Lee, S. J. *Compos. Struct.* **2012**, *94*, 1236.
44. Muric, N.; Compston, P.; Stachurski, Z. H. *Compos. Part A* **2011**, *42*, 320.
45. Fu, S. Y.; Feng, X. Q.; Lauke, B.; Mai, Y. W. *Compos. Part B* **2008**, *39*, 933.
46. Jena, H.; Satapathy, A. K. *Int. J. Manuf. Mater. Sci.* **2012**, *2*, 27.
47. Antunes, P.; Ramalho, A.; Carrilho, E. *Mater. Des.* **2014**, *61*, 50.
48. Salvador, M. D.; Amigo, V.; Sahuquillo, O.; Antolinos, C. M.; Segovia, F.; Vicente, A. In Proceedings of 11th European Conference on Composite Material, **2004**.
49. Haameem, M. J. A.; Abdul Majid, M. S.; Afendi, M.; Marzuki, H. F. A.; Fahmi, I.; Gibson, A. G. *Compos. Struct.* **2016**, *136*, 1.
50. Mulinari, D. R.; Baptista, C. A. R. P.; Souza, J. V. C.; Voorwald, H. J. C. *Proc. Eng.* **2011**, *10*, 2074.
51. Lopez, F. A.; Martin, M. I.; Alguacil, F. J.; Rincon, J. M.; Centeno, T. A.; Romero, M. *J. Anal. Appl. Pyrolysis* **2012**, *93*, 104.
52. Bansal, R. K.; Mittal, J.; Singh, P. *J. Appl. Polym. Sci.* **1989**, *37*, 1901.
53. Green, K. J.; Dean, D. R.; Vaidya, U. K.; Nyairo, E. *Compos. Part A* **2009**, *40*, 1470.
54. Mohan, T. P.; Kanny, K. S. *Compos. Part A* **2011**, *42*, 385.
55. Ke, F.; Jiang, X.; Xu, H.; Ji, J.; Su, Y. *Compos. Sci. Technol.* **2012**, *72*, 574.
56. Pérez, E.; Bernal, C.; Piacquadio, M. *Appl. Surf. Sci.* **2012**, *258*, 8940.